Clays and Clay Minerals, Vol. 53, No. 2, 162–170, 2005.

CHARACTERISTICS OF THE MINERALS ASSOCIATED WITH GOLD IN THE SHEWUSHAN SUPERGENE GOLD DEPOSIT, CHINA

HANLIE HONG* AND LIYUN TIE

The Center for Material Research and Testing, Wuhan University of Technology, Wuhan, Hubei, 430070, P.R. China

Abstract—The mineralogical properties of goethite and clay minerals from the Shewushan supergene gold deposit have been studied using X-ray diffraction (XRD) and transmission electron microscopy (TEM). These results show that in the weathering zone of the Shewushan supergene gold deposit the mineral assemblage is mainly composed of quartz, kaolinite, halloysite, minor illite and goethite. The coexistence of these minerals is apparently indicative of weak laterization. The Al content in goethite from XRD data is ~10.0%, suggesting formation by weak desilicification. Observation by TEM shows that the flakes of clay minerals with larger particle size usually have extremely rounded outlines, indicating intensive dissolution of clay minerals. Halloysite is derived from the decomposition of kaolinite and the micrographs of curling, tubular, and club-shaped halloysite strongly suggest significant hydration and thus a water-saturated environment. Both the XRD data of goethite and the micrographs of the clay minerals show that the environment in Shewushan is characteristic of high [H_2O] activity and high [SiO_2] activity. The high dynamic hydraulic conditions may facilitate the downward migration of the primary gold particles during their mechanical concentration, resulting in the accumulation of gold in the lower portion near the water table.

Key Words—Clay Minerals, Crystallinity, Goethite, Lateritization, Micrograph, Supergene Gold Deposit, Weathering Zone.

INTRODUCTION

Since the discovery of the Boddington lateritic gold deposit in Western Australia (Davy, 1979; Davy and El-Ansary, 1986), intensive prospecting for lateritic gold deposits has been undertaken in many countries. Investigations revealed that a number of lateritic gold deposits are situated in the tropics where extensive lateritic terrains existed during the Tertiary and Recent times in inner tropical morphoclimate zones covered by dense rain forests. Laterites were formed in places such as the Amazon region and West Africa (Da Costa, 1993; Zang and Fyfe, 1993). However, in China, the first weathering-related gold deposit, at Shewushan, Hubei (Figure 1), was found in 1989, and subsequently, a number of similar supergene gold deposits were found at other locations in south China, *e.g.* in Yunnan, Hunan and Guizhou. However, both the climate and the tectonic settings in south China are different from the area where typical lateritic gold deposits are located. For example, the climate is warm and humid in the Shewushan area. The mean annual rainfall is ~1100 mm, falling mainly between April and October, and the mean average temperature is 18ºC, with the mean 4.1ºC during the coldest month (January) and 29.2ºC during the warmest month (July). The landscape consists of hills covered with evergreen trees and bushes and comprises relatively flat aggraded and coalesced alluvial fans, with the base level of erosion 20 m above mean sea level. On the other hand, the intensive tectonic movement during the Cenozoic limited the development of an erosional plain, and most of the bedrock is primary carbonates. As a result, the particle size of the gold in the weathering profile is extremely small; most grains are <0.02 μm in size and occur at the rims of clay mineral grains (Hong *et al*., 1999).

Previous studies of the Shewushan gold deposit have mainly focused on the geological conditions, geochemical characteristics, and genetic model of this type of weathering-related gold deposit (Li, 1993; Yu, 1994; Hong, 2000). However, studies of the mineralogical characteristics of the associated minerals may be even more important: (1) the small particle size of the gold creates difficulties in understanding the gold mineralogy and the mechanism of gold mineralization; (2) the mineralogical characteristics of the associated minerals are actually the products of persistent weathering and are indicative of laterization and gold mineralization. The aims of this study are to acquire a greater understanding of the mineralogical characteristics of clay minerals in the weathering zone and thereby the laterization and the conditions producing the gold mineralization.

GEOLOGICAL SETTING AND THE WEATHERING PROFILE

Geological setting

The geological setting of the Shewushan area has been studied intensively (Li, 1993; Yu, 1994). The results show that an anticline is situated beneath the

* E-mail address of corresponding author:
honghl@public.wh.hb.cn
DOI: 10.1346/CCMN.2005.0530206

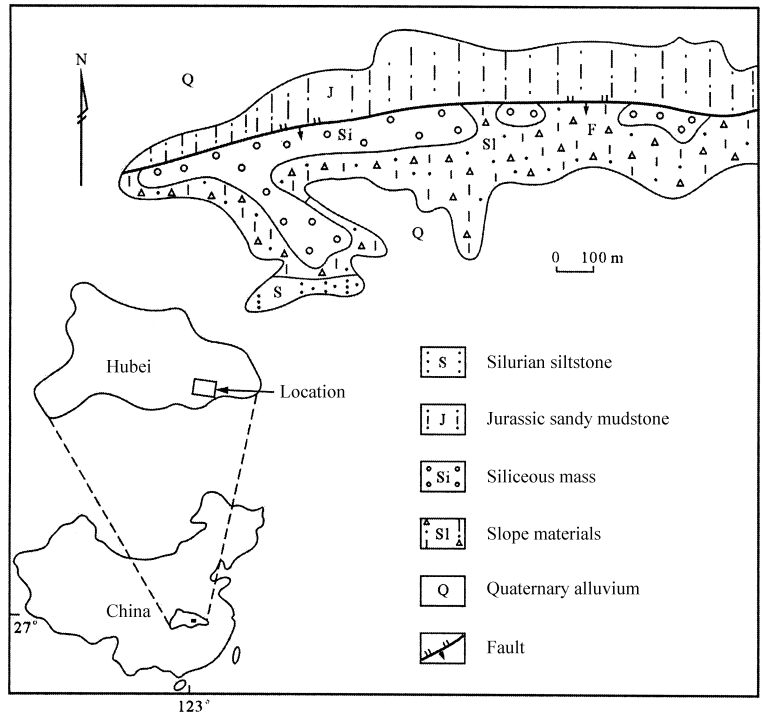

Figure 1. A generalized map showing the location and the geology of the Shewushan supergene gold deposit.

deposit with the axis of Cambrian to Ordovician limestone or dolostone and limbs of Silurian to Jurassic mudstone with limestone bands (Figure 2). There is a set of high-angle thrust folds trending east–west within the axis and the limbs. The gold deposit occurs in the Shewushan thrust zone, a major east–west-trending structure. It cuts across the center of the Shewushan gold deposit which was the conduit of epithermal mineralization, now in the weathering zone, resulting from the mineralized tectonic melange. Hypogene gold mineralization occurs discontinuously in a number of high-angle folded thrusts containing mainly carbonate and minor sulfide (usually <5%). The gold content of unweathered rock rarely exceeds 1.0 μg/g, most of which ranges from 0.1 μg/g to 1.0 μg/g, with a mean 0.6 μg/g. Gold occurs within small Ag-bearing particles, nm-scale in size, adsorbed at the edges of illite and kaolinite, and partly within the auropyrite (Wang and Yang, 1992; Li, 1993). Stratigraphic studies of the Shewushan area indicate that the Cretaceous to Tertiary is missing in the area; erosion at Shewushan has taken place since the

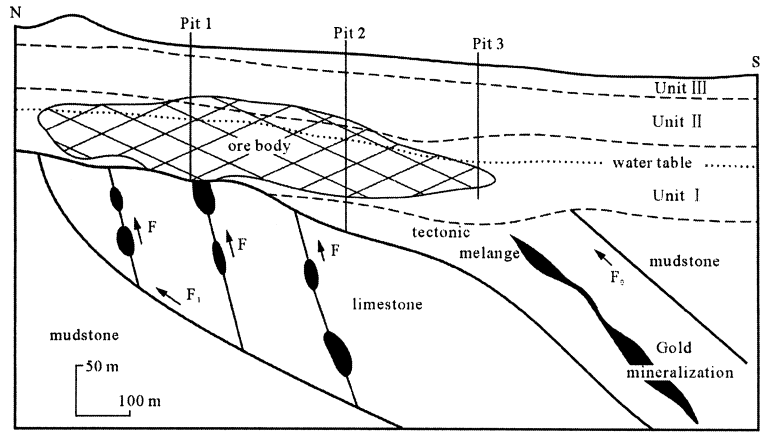

Figure 2. A generalized weathering profile of the Shewushan supergene gold deposit showing the lithology, structure and gold distribution.

https://doi.org/10.1346/CCMN.2005.0530206 Published online by Cambridge University Press

Cretaceous, with upwards and downwards movement of the water table, perhaps due to seasonal changes, producing a redox environment and hence causes the dissolution and deposition of minerals in the weathering profile during the weathering process (Yu, 1994).

Characteristics of the weathering zone

The weathering zone in the mineralized tectonic melange can be divided into three units, saprolite (Unit I), mottled clay (Unit II), and gravelly clay and massive silica (Unit III) from the fresh rocks to the surface, as shown in Figure 2. Saprolite forms the lowermost unit of the regolith which locally preserves the structure and texture of the parent rock. It consists of brown to red-brown clay and gravelly clay and is composed of illite, kaolinite, carbonate, quartz, Fe and Mn oxides and rare sulfide and gypsum. The saprolite is the main gold-bearing horizon, having a gold content ranging from 0.34 to 19.49 μg/g. Saprolite grades upwards into the mottled clay in which the primary rock fabric is poorly preserved. The mineral assemblage differs from that of saprolite. It lacks carbonates, sulfide and Fe and Mn oxides. Most of the Fe and Mn oxides were carried away via groundwater penetrating downwards during persistent lixiviation, and the clay minerals were whitened. As a result, light-colored spots, nodules and net-like veins are prominent in this part. Clay minerals occur as white lenticular bodies in some places. The gold content of this unit ranges from 0.2 to 3.4 μg/g. Gravelly clay and massive silica form the uppermost horizon. The mineral assemblage consists of quartz, chalcedony, kaolinite, halloysite, barite and minor Fe and Mn oxides. Due to resistance to weathering, huge blocks of massive silica project to the surface. The gold content of the unit ranges from 0.0 to 2.0 μg/g.

Clay minerals occur widely in the weathering zone, and the mineral composition appears to vary with depth in the weathering profile. In the upper part of the weathering profile, the clay minerals are mainly kaolinite and halloysite, and minor illite. These are red because of contamination with Fe oxides and hydroxides and coatings on their surfaces. In the middle part of the profile, the main clay minerals are kaolinite and illite, and the halloysite content is smaller than in the upper part. Generally, the clay minerals are white to light yellow in color as a result of persistent lixiviation. In the lower part of the profile, the clay minerals comprise mainly illite and kaolinite, the kaolinite content decreasing while the illite content increases. Halloysite is extremely rare in the lower part of the weathering zone (Yu, 1994; Hong, 2000).

EXPERIMENTAL METHODS

Sample preparation

Samples were collected from pits in the upper portion of the weathering zone in the ore deposit with a gold content of 3.6 μg/g and a total weight of ~5 kg. Samples were oven dried at 60ºC for 24 h, and then crushed and ground to pass a <200 mesh. The goethite separate was collected using panning. A clay minerals separate with a grain size <5 μm and a total mass of ~5 g was prepared using the pulverized sample and a method of precipitation. (The grain size of the clay minerals was estimated from the rate of settling.) This separate was used for TEM observation and XRD analysis.

X-ray diffraction analysis

Powder diffraction analyses were carried out on a RIKAGU D/MAX-IIIA diffractometer with Ni-filtered CuKα radiation using 35 kV X-ray tube voltage and 35 mA tube current, 1º divergence slit, 1º anti-scatter slit and 0.3 mm receiving slit. The goethite samples were ground with an agate pestle in a small agate mortar to ~20 μm in particle size and then the goethite sample, as well as the clay minerals sample, were mounted onto a sample plate. The XRD patterns were collected from 2 to 65º2θ at a scan rate of 2º2θ/min. The Al^{3+} content in the goethite structure and the Hinckley index of kaolinite were calculated from these data.

As the ionic radius of Al^{3+} is 0.53 Å and that of Fe^{3+} is 0.65 Å (Shannon and Prewitt, 1969) substitution of Al^{3+} for Fe^{3+} in the crystal structure of goethite will result in a change of cell parameters and the average size of the unit-cell will decrease when Al substitutes for Fe in the goethite structure. The Al^{3+} content in the goethite structure is calculated according to the method proposed by Schulze (1984), which can be obtained by solving the regression line equation between Al^{3+} content and the c dimension of goethite, as follows:

$$\text{mole \% Al} = 1730 - 572.0c$$

where the c dimension can be calculated according to the d values of the 110 line and the 111 line of goethite by the formula:

$$c = [(1/d(111))^2 - (1/d(110))^2]^{-1/2}$$

The Hinckley index, reflecting the defect structure of kaolinite, was calculated according to the ratio of the sum of the heights of the peaks $1\bar{1}0$ and $11\bar{1}$ measured from the inter-peak background to the height of the $1\bar{1}0$ peak measured from the general background (Hinckley, 1963).

TEM analysis

The clay minerals sample was dispersed in the ultrasonic equipment for ~15 min, and was then collected with a copper net and dried under an infrared light. The TEM observation of clay minerals was performed using an Hitachi 800 analytical electron microscope equipped with a TN-5500 energy dispersion spectrometer (EDS). The instrument was operated at 120 kV with a beam current from 20 to 30 μA. The EDS element analysis was used to identify the mineral

https://doi.org/10.1346/CCMN.2005.0530206 Published online by Cambridge University Press

components qualitatively, especially those of small particle size with irregular outline.

RESULTS

X-ray diffraction analysis

The XRD patterns of both the clay minerals and the goethite sample are shown in Figure 3, part a of which confirms that the goethite separate contains mainly goethite, with minor quartz and kaolinite (and/or halloysite). As shown, the *d* value of the 110 line of goethite is 4.170 Å and the *d* value of the 111 line is 2.439 Å; therefore, the *c* value was calculated, according to the formula, as 3.007 Å, and the ratio of Al^{3+} to Fe^{3+} was calculated, using the regression line equation, to be ~10.0%.

Figure 3b indicates that the clay minerals separate consists of kaolinite (or halloysite) and illite, with minor quartz. From the intensity of the diffraction lines, it can be inferred that there is only minor illite in the sample; however, the halloysite peaks are significantly overlapped by those of kaolinite, hence both kaolinite and halloysite cannot be easily distinguished from each other by XRD. The heights of the $1\bar{1}0$ and $11\bar{1}$ peaks were measured as mentioned above, and the Hinckley index of the kaolinite was calculated to be ~0.81.

TEM analysis

Transmission electron microscopy images of the clay minerals (Figure 4) show that most of the kaolinite crystals show poorly developed hexagonal to pseudo-hexagonal plates slightly elongated in one direction, exhibiting irregular outline or ragged edges, as shown in Figure 4a,b,d. Some kaolinite grains have been rounded because of intensive dissolution during weathering (Figure 4b,c,g). In general, the majority of the basal (001) plane appears smooth or flat, and other surfaces such as (110) and (010) are poorly developed. The particle size of kaolinite in basal plane dimension ranges from 0.25 to 5.25 μm according to statistics. In some cases, minor kaolinite crystals have flat surfaces in lateral dimension, which are clearly defined and at right angles to the basal (001) surface with a thickness of

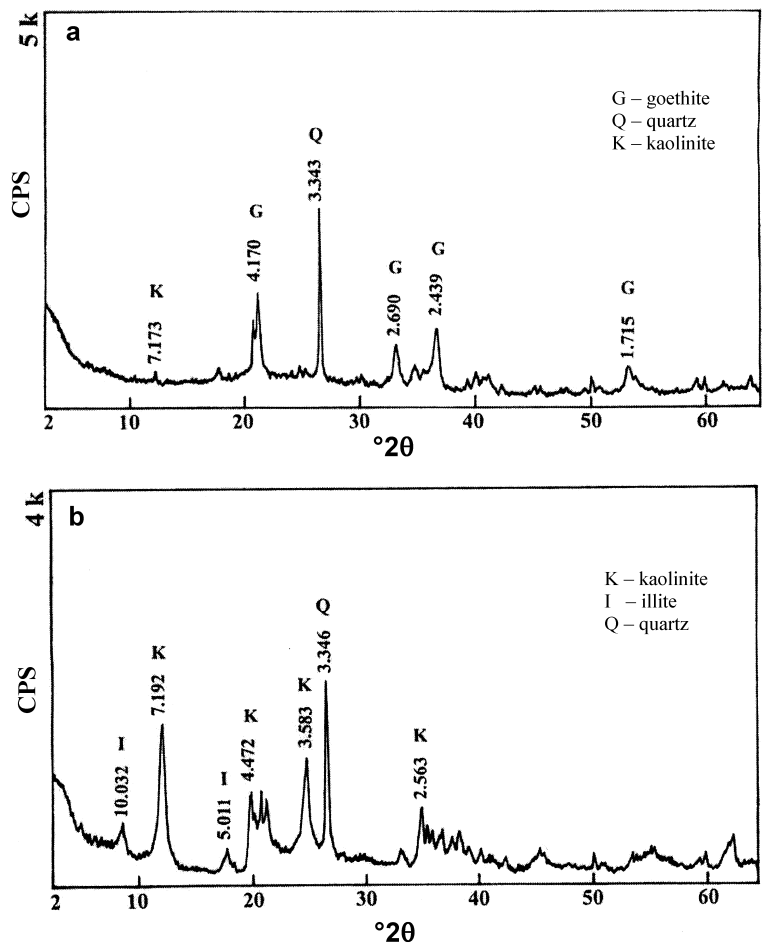

Figure 3. The XRD patterns of goethite and clay minerals from the Shewushan supergene gold deposit: (a) goethite separate showing the *d* values (Å) of the strong lines of goethite; (b) clay minerals separate showing the mineral composition of kaolinite (or/and halloysite), illite and minor quartz.

https://doi.org/10.1346/CCMN.2005.0530206 Published online by Cambridge University Press

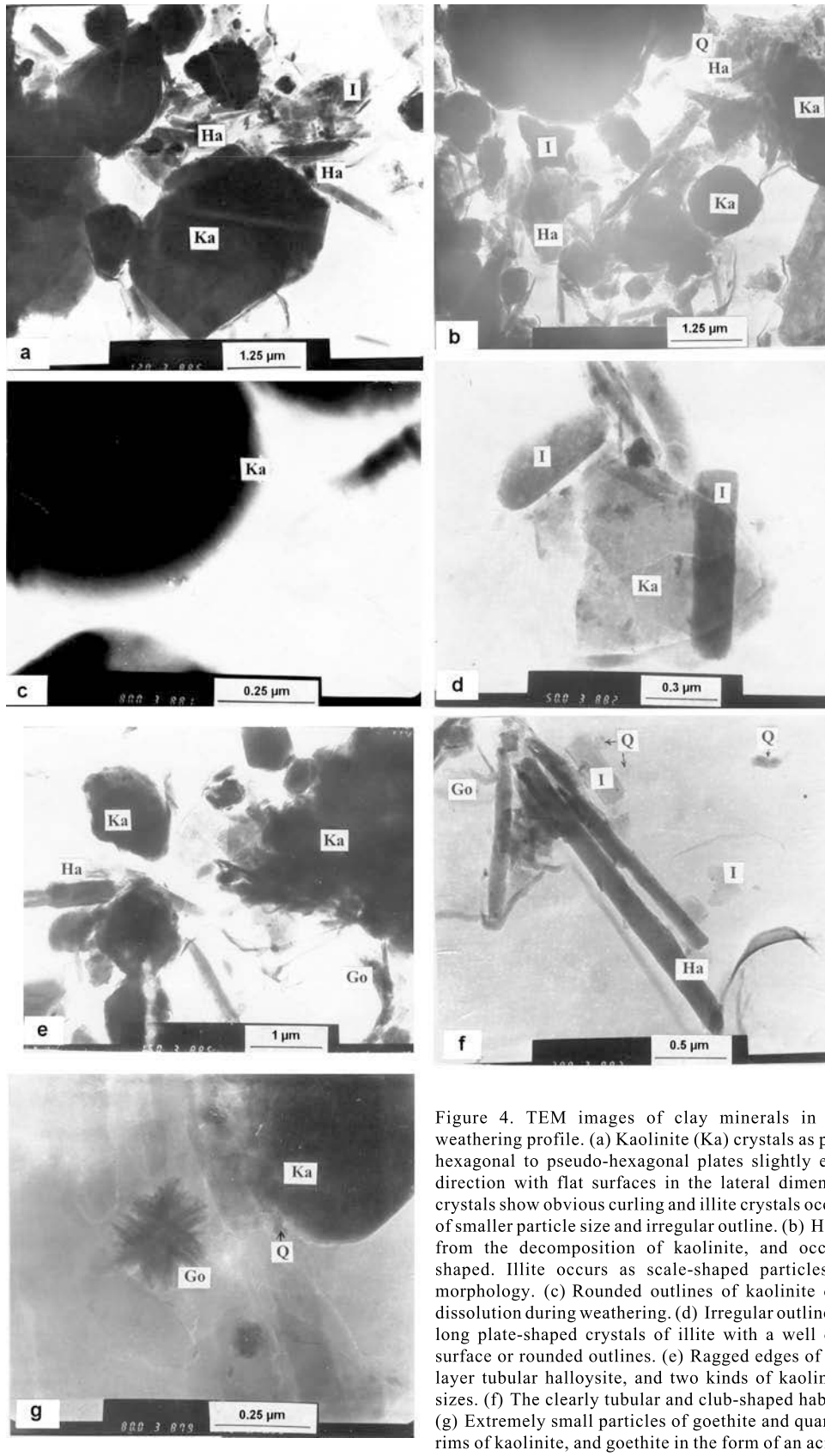

Figure 4. TEM images of clay minerals in the Shewushan weathering profile. (a) Kaolinite (Ka) crystals as poorly developed hexagonal to pseudo-hexagonal plates slightly elongated in one direction with flat surfaces in the lateral dimension. Halloysite crystals show obvious curling and illite crystals occur as aggregates of smaller particle size and irregular outline. (b) Halloysite derived from the decomposition of kaolinite, and occasionally plate-shaped. Illite occurs as scale-shaped particles with irregular morphology. (c) Rounded outlines of kaolinite due to intensive dissolution during weathering. (d) Irregular outline of kaolinite and long plate-shaped crystals of illite with a well developed (010) surface or rounded outlines. (e) Ragged edges of kaolinite, multi-layer tubular halloysite, and two kinds of kaolinites of different sizes. (f) The clearly tubular and club-shaped habits of halloysite. (g) Extremely small particles of goethite and quartz on the crystal rims of kaolinite, and goethite in the form of an acicular aggregate.

https://doi.org/10.1346/CCMN.2005.0530206 Published online by Cambridge University Press

~0.15 μm (Figure 4a). Energy dispersive spectroscopy evidence shows that the crystal rims of kaolinite contain goethite and quartz (Figure 4b,e,g).

Halloysite is closely associated with kaolinite. Halloysite has three different morphologies: (1) curling particles, as shown in Figure 4a; (2) tubular or club-like (Figure 4f), and multi-layer tubular particles (Figure 4e); (3) plate-shaped particles, as shown in Figure 4b. Kaolinite and halloysite have similar chemical compositions, and EDS cannot distinguish between them. Therefore, this kind of halloysite was determined not only by EDS element analysis, but also by excluding kaolinite according to the apparent outline of kaolinite flakes. Measurement by TEM indicates that tubular or club-shaped halloysite crystals have lengths ranging from 0.42 to 1.67 μm, and diameters from 0.08–0.16 μm, while the plate-shaped halloysite crystals are 0.15–0.50 μm long and 0.08–0.12 μm wide.

We observed four different morphologies for illite. (1) Some grains show perfect crystalline character, occurring as long plate-shaped crystals with a well developed (010) surface (Figure 4d). (2) Some illite crystals also show elongated plates with rounded edges (Figure 4d). (3) As shown in Figure 4b, illite crystals occur as scale-shaped particles with irregular crystal shapes. (4) Less commonly, crystals occur as aggregates with smaller particle size and irregular outline (Figure 4a). On the whole, illite can be largely divided into two groups according to its particle size, the larger illite particles with long plate-shaped outline are 0.4–1.0 μm long and 0.1–0.3 μm wide, and the smaller illites with irregular outline have a particle size from 0.1 to 0.6 μm.

DISCUSSION

X-ray diffraction

Goethite is the most common of the Fe oxide minerals in soils and occurs in almost every type of soil environment (Schwertmann and Taylor, 1977), derived from the intensive weathering of Fe-bearing minerals under a warm and humid climate. The ionic substitution of Al for Fe in goethite is well known (Norrish and Taylor, 1961; Davey *et al*., 1975; Torrent *et al*., 1980; Fitzpatrick and Schwertmann, 1981; Schwertmann and Carlson, 1994), and Al substitution ranges up to 33 mol.%. Fitzpatrick and Schwertmann (1981) showed that the amount of Al substitution in goethite varies among different soil environments and that Al substitution may be an indicator of pedogenic conditions.

In most natural systems, aluminous goethites are associated with kaolinite. The presence of kaolinite in soils or weathering profiles may induce changes in the Al contents of the associated aluminous goethite. The Al content of aluminous goethite at equilibrium with kaolinite decreases when water activity or silica activity increases (Trolard and Tardy, 1989). Hence, goethites are poorer in Al in lowland and hydromorphic soils than in Ultisols located at the top of the profile. For a given activity of water, the extent of substitution of Fe by Al in aluminous goethite decreases with increase in silica activity. This indicates that in the weathering zone with weak desilicification, where there has been a greater degree of silica activity, goethite will exhibit a smaller Al^{3+}/Fe^{3+} ratio, and inversely, in the weathering zone with intensive desilicification, where there has been a lesser degree of silica activity, goethite will show a greater Al^{3+}/Fe^{3+} ratio. Therefore, the Al^{3+}/Fe^{3+} ratio of goethite may reflect the degree of desilicification and water conditions in the weathering zone, and thus it is indicative of the degree of laterization and site where goethite formed in the weathering profile. The Al^{3+}/Fe^{3+} ratio of the goethite from Shewushan is ~10.0%, suggesting that goethite in the weathering zone was generated by weak desilicification in a water-saturated environment. Thus, it can be inferred that the laterization at Shewushan is weakly developed.

The XRD patterns of the clay minerals show that the clay minerals comprise mainly kaolinite (or/and halloysite) and minor illite (Figure 3b). The lines of kaolinite are overlapped by those of halloysite in the XRD pattern. However, from TEM measurements, we can tell that the amount of halloysite is very small. From the XRD profile, the Hinckley index of kaolinite is ~0.81, suggesting that the kaolinite in the weathering zone has quite low crystallinity. Kaolinite is the dominant clay mineral, widely distributed in lateritic soils and weathering zones. The degree of crystallinity of kaolinite reflects the stacking sequence of layers, the shifts between adjacent layers by $\pm nb/3$, the frequency of defects, largely caused by geological conditions of formation, transport, or deposition, and therefore is related to the geological and geochemical environment (Brindley, 1986). In fact, kaolinite can contain small amounts of Fe substituting for Al. It has been shown that an increase in the Fe content is accompanied by a reduction in the crystallinity and an increase in the disorder of kaolinite. In the weathering zone at Shewushan, intensive oxidation and lixiviation resulted in a weak acid to weak alkaline groundwater, thus increasing the solubility of Si and Al, and in particular increasing the activity of Fe^{3+}. Thus, kaolinite in this environment has low crystallinity.

Micrographs of the clay minerals

Tardy and Nahon (1985) pointed out that, in the permanently humid tropical red or yellow lateritic soils in which kaolinite dominates, goethite is the dominant ferric mineral and the typical paragenesis is quartz, kaolinite and goethite. However, in the Shewushan weathering profile, TEM observations reveal that kaolinite, halloysite, illite, goethite and quartz coexist in the lateritic soil. Kaolinite and halloysite are two of the most

https://doi.org/10.1346/CCMN.2005.0530206 Published online by Cambridge University Press

abundant supergene minerals. In particular, halloysite is usually produced due to intensive lixiviation in an acidic environment. However, illite is stable in neutral to alkaline solutions. The assemblage of kaolinite, halloysite, illite, goethite and quartz is indicative of a weakly developed laterization, in good agreement with the results from the mineralogical analysis of goethite.

Beneath the weathering zone is the mineralized tectonic melange containing rock fragments of different kinds of lithology and chronology, consisting mainly of argillaceous limestone, limestone, and argillite (Li, 1993). These rocks may transform into clay minerals during the weathering process. Thin-section examination has shown that the argillaceous limestone and the argillite contain significant amounts of illite, and locally the argillite consists entirely of illite, a common aluminosilicate, which is unstable and liable to decompose in the weathering environment. Decomposition of illite will produce Si oxide and Al oxide which may be soluble in groundwater or occur as Si-, Al-colloids, and the concentrations of Si and Al will gradually increase with the weathering process, when the concentrations of Si and Al are large enough for crystallization of kaolinite which will deposit in the lower part of the weathering profile. SiO_2 and Al_2O_3 colloids usually crystallize as kaolinite and halloysite; the reaction equation is as follows (Ren, 1992):

$$2\underset{\text{(illite)}}{KAl_5Si_7O_{20}(OH)_4} + 2H^+ + 2HCO_3^- + 13H_2O \rightarrow 5\underset{\text{(kaolinite)}}{Al_2Si_2O_5(OH)_4} + 4H_4SiO_4 + 2KHCO_3$$

The reaction product $KHCO_3$ is soluble in water and will be carried away by penetrating groundwater; H_4SiO_4, mainly in colloidal form, will be retained by the clay minerals for adsorption and finally transform into quartz due to dewatering. This kind of quartz is particularly small in size and is closely associated with clay minerals.

Previous works have shown that the unweathered gold-bearing rock consists of ~16% clay minerals (illite and minor kaolinite), 58% carbonate (calcite and minor dolomite), 20% quartz, 3% pyrite and minor barite (Wang and Yang, 1992). However, in the weathering profile, the illite content increases with depth while the halloysite content decreases from the top to the bottom of the weathering profile. In the uppermost part of the weathering zone in particular, only minor illite (~8% of the clay mineral separate) is found, and the clay minerals mainly comprise kaolinite (47%) and halloysite (45%). On the contrary, in the lower portion of the profile, the clay minerals largely comprise illite and kaolinite. Therefore, from the bottom to the upper part of the weathering profile, the illite content decreases gradually due to weathering, and the amount of kaolinite increases relative to illite during the weathering process. Michel (1987) investigated the weathering profile at Mato Grosso, Brazil and also showed that, in the *in situ* lateritic soil from overlying Precambrian schists of the Cuiaba Group, illite alteration produces minor kaolinite.

Observation by TEM also shows that kaolinite flakes with larger particle size usually have very round outlines, suggesting that intensive dissolution of clay minerals has taken place in the Shewushan environment. The dissolution of clay minerals produces SiO_2 which will crystallize as quartz of small particle size. On the other hand, oxidation will also produce Fe oxide or hydroxide which will be mainly accumulated in the lower portion of the weathering zone due to the changes in both the dynamic hydraulic conditions and the solution conditions of the groundwater, and the Fe content will gradually increase with weathering. Some of the Fe crystallizes as goethite, which usually takes on the habit of an acicular aggregate with very small particle size (Figure 4g). Some may occur as X-ray amorphous Fe oxide or hydroxide. Iron materials are usually adsorbed onto the surface of kaolinite or coated on the surface of kaolinite, thereby resulting in the intensive Fe contamination of the clay minerals.

Under TEM observation, most of the halloysite crystals appear to have curling, tubular and club-shaped morphologies, indicating the significant hydration and thus the water-saturated environment. Halloysite is associated with kaolinite – as shown in Figure 4b, at the crystal rims of kaolinite where there is a cluster of fine-grained halloysite which was clearly derived from the decomposition of kaolinite. The weathering zone at Shewushan was derived from the tectonic melange, which has a loose texture and well developed fissures, and favors the penetration of groundwater. Thus, kaolinite will be hydrated into halloysite due to persistent lixiviation of groundwater. Therefore, in the weathering zone, the kaolinite of larger particle size and with irregular outline may be derived from the dissolution of the original kaolinite in the bedrock due to weathering, and the kaolinite of smaller particle size and euhedral hexagonal plates may have formed during weathering.

Gold in the weathering zone

The presence of gold in lateritic soils commonly results from a high concentration factor during laterization (Mann, 1984). However, the origin and the mechanism of gold concentration may differ depending on each specific geological setting. In permanently humid tropical red or yellow lateritic soils the typical paragenesis is quartz, kaolinite and goethite. However, in the Shewushan weathering profile, the typical paragenesis is kaolinite, halloysite, illite, goethite and quartz. On the other hand, the lower Al^{3+}/Fe^{3+} ratio of the goethite suggests that goethite in the weathering zone was generated in a weak desilicification and water-saturated environment. The characteristics of the minerals indicate a weakly developed laterite.

https://doi.org/10.1346/CCMN.2005.0530206 Published online by Cambridge University Press

At Shewushan, secondary gold grains present in the weathering profile exhibit unique characteristics of small particle size and high purity. Studies of pan concentrates and polished sections demonstrated that gold particles are optically invisible and hence are too small for study of their morphology. Transmission electron microscopy and electron probe microanalysis indicate that most of the gold occurs as extremely small particles in nanometer scale adsorbed at the crystal edges of kaolinite and illite, and minor gold is intermixed with goethite. The largest grain found in the former study was ~0.6 μm in diameter, and EDS analyses showed that gold grains from the weathering zone are of very high purity (Hong *et al*., 1999). In Western Australia all the secondary gold in the saprolite zone of supergene gold deposits has a total absence of impurities of other elements (Mann, 1984; Webster, 1986). Interstitial grains and droplets of gold with high purity have been found in the Boddington gold deposit (Monti, 1987). This pure gold is generally concentrated in flat-lying zones of Fe oxide associated with the paleo- and present water table. The characteristics of supergene gold at Shewushan are quite similar to those of the Boddington gold deposit in Western Australia. The only difference is the degree of weathering development. At Boddington, extensive tropical weathering has produced a well developed bauxitic laterite, which consists mainly of gibbsite, hematite, goethite, quartz and kaolinite (Davy and El-Ansary, 1986), whereas at Shewushan, the weathering zone is only a weakly developed, immature laterite.

Hypogene gold at Shewushan is present as both nm-scale native Ag-bearing gold particles, adsorbed at the crystal rims of illite and kaolinite, and as auriferous pyrite. Supergene gold is present only in the native form, occurring closely related to kaolinite and illite, and Fe oxides and hydroxides. Oxidation of pyrite at Shewushan led to the release of of gold and accumulation by clay minerals and Fe oxides and hydroxides. The secondary gold intermixed with Fe oxides and hydroxides has been interpreted as the product of the oxidation of gold-bearing pyrite (Bowell, 1992). Meanwhile, the weathering process would also result in the Ag depletion of the primary gold particles in the weathering profile (Mann, 1984; Webster, 1986). The primary gold grains at Shewushan are particularly small, promoting the Ag-depletion reactions during the weathering process. Thus, the secondary gold at Shewushan is of very high purity. According to the mineral characteristics of the associated clay minerals and goethite, the Shewushan environment was water saturated. The unweathered gold-mineralization rocks consisted of tectonic melange with a characteristically high porosity. Therefore, the weathering zone at Shewushan would have a high dynamic hydraulic conductivity and intensive downward migration of the primary gold particles would be expected during their mechanical concentration, and finally, most of the gold accumulated at the lower portion near the water table where both the dynamic hydraulic conditions and the Eh-pH conditions changed abruptly.

CONCLUSIONS

One of the primary observations from this study is that in the Shewushan environment, the mineral assemblage of the weathering zone is mainly composed of quartz, kaolinite, halloysite, minor illite and goethite. The assemblage of these minerals in the weathering zone is apparently indicative of weak laterization of Shewushan weathering zone and therefore it is an immature lateritic horizon in comparison with a typical tropical laterite.

The Hinckley index of kaolinite is ~0.81 which suggests that the kaolinite in the weathering zone has quite low crystallinity. Observation by TEM shows that the flakes of clay minerals with larger particle size usually have extremely round outlines, suggesting that intensive dissolution of clay minerals takes place in the Shewushan environment. The TEM results also indicate that halloysite is derived from the decomposition of kaolinite in the weathering zone. The micrographs of curling halloysite provide further evidence of the water-saturated environment at Shewushan. The Al content in goethite, as calculated from XRD data, is ~10.0%, showing that goethite in the weathering zone at the Shewushan supergene gold deposit was generated in weak desilicification and high water-activity conditions.

Both the XRD data of goethite and the micrographs of the clay minerals show that the environment in Shewushan is characteristic of high [H_2O] activity and high [SiO_2] activity during the weathering process. The high dynamic hydraulic conductivity may facilitate the downward migration of the primary gold particles during their mechanical concentration, resulting in the accumulation of gold near the water table.

ACKNOWLEDGMENTS

This work was supported by the Natural Science Foundation of China (NSFC), allotment grant number 40172017. The authors wish to thank Dr X.M. Zhang and X.Y. Hu for sample preparation, Dr X.W. Liu for the SEM observations, Dr J.F. Qian for the XRD measurement, and Prof. K.D. Stephen for improving the English. The authors are also grateful to Prof. R.Y. Yu and C.Q. Peng for their helpful discussion, and especially the anonymous reviewers, the Associate Editor Crawford Elliott and Dr D.C. Bain for their valuable comments and suggestions.

REFERENCES

Bowell, R.J. (1992) Supergene gold mineralogy at Ashanti, Ghana: Implications for the supergene behaviour of gold. *Mineralogical Magazine*, **56**, 545–560.

Da Costa M.L. (1993) Gold distribution in lateritic profiles in South America, Africa, and Australia: applications to geochemical exploration in tropical regions. *Journal of*

Geochemical Exploration, **47**, 143–163.
Davey, B.G., Russell, J.D. and Wilson, M.J. (1975) Iron and clay minerals and their relation to colors of red and yellow Podzolic soils near Sydney, Australia. *Geoderma*, **14**, 125–138.
Davy, R. (1979) Geochemical exploration, Saddleback greenstone belt, Western Australia. *Western Australia Geological Survey*, 1979(8).
Davy, R. and El-Ansary, M. (1986) Geochemical patterns in the laterite profile at the Boddington gold deposit, Western Australia. *Journal of Geochemical Exploration*, **26**, 119–144.
Fitzpatrick, R.W. and Schwertmann, U. (1981) Al-substituted goethite – an indicator of pedogenic and other weathering environments in South Africa. *Geoderma*, **27**, 335–347.
Hinckley, D.N. (1963) Variability in "crystallinity" values among the kaolin deposits of the coastal plain of Georgia and South Carolina. *Clays and Clay Minerals*, **11**, 229–235.
Hong, H.L. (2000) Behaviour of gold in the weathered mantle at Shewushan, Hubei, China. *Journal of Geochemical Exploration*, **68**, 57–68.
Hong, H.L., Wang, Q.Y., Chang, J.P., Liu, S.R. and Hu, R. (1999) Occurrence and distribution of invisible gold in the Shewushan supergene gold deposit China. *The Canadian Mineralogist*, **38**, 1525–1531.
Li, S.S. (1993) The ore geology and genetic model for Shewushan lateritic gold deposit. *Geology and Exploration*, **29**, 12–15 (in Chinese).
Mann, A.W. (1984) Mobility of gold and silver in lateritic weathering profiles: Some observations from Western Australia. *Economic Geology*, **79**, 38–49.
Michel, D. (1987) Concentration of gold in in situ laterites from Mato Grosso. *Mineralium Deposita*, **22**, 185–189.
Monti, R. (1987) The Boddington lateritic gold deposit, Western Australia: A product of supergene enrichment processes: Nedlands, *University of Western Australia Geology Department and University Extension Publication*, **11**, 355–368.
Norrish, K. and Taylor, R.M. (1961) The isomorphous replacement of iron by aluminium in soil goethites. *Journal of Soil Science*, **12**, 294–306.
Ren, L.F. (1992) *Clay Minerals and Clay Rock.* Geological Press, Beijing, pp. 18–74 (in Chinese).
Schulze, D.G. (1984) The influence of aluminum on iron oxides: VIII. Unit-cell dimensions of Al-substituted goethites and estimation of Al from them. *Clays and Clay Minerals*, **32**, 36–44.
Schwertmann, U. and Carlson, L. (1994) Aluminum influence on iron oxides: XVII. Unit-cell parameters and aluminum substitution of natural geothites. *Soil Science Society of America Journal*, **58**, 256–261.
Schwertmann, U. and Taylor, R.M. (1977) *Iron Oxides in Minerals in Soil Environments* (J.B. Dixon and S.B. Weed, editors). Soil Science Society of America, Madison, Wisconsin, pp. 145–180.
Shannon, R.D. and Prewitt, C.T. (1969) Effective ionic radii in oxides and fluorides. *Acta Crystallographica*, **B25**, 925–946.
Tardy, Y. and Nahon, D. (1985) Geochemistry of laterites, stability of Al-goethite, Al-hematite, and Fe^{3+}-kaolinite in bauxites and ferricretes: an approach to the mechanism of concentration formation. *American Journal of Science*, **285**, 865–903.
Torrent, J., Schwertmann, U. and Schulze, D.G. (1980) Iron oxide mineralogy of some soils of two river terrace sequences in Spain. *Geoderma*, **23**, 191–208.
Trolard, F. and Tardy, Y. (1989) A model of Fe^{3+}-kaolinite, Al^{3+}-goethite, Al^{3+}-hematite equilibria in laterites. *Clay Minerals*, **24**, 1–21.
Wang, T. and Yang, M.A. (1992) A preliminary study on the occurrence of gold in primary ore from Shewushan gold deposit. *Hubei Geology*, **6**(2), 40–46 (in Chinese).
Webster, J.G. (1986) The solubility of gold and silver in the system Au-Ag-S-O_2-H_2O at 25ºC and 1 atm. *Geochimica et Cosmochimica Acta*, **50**, 1827–1845.
Yu, R.Y. (1994) Some new ideas of the loose layers in Shewushan supergene gold deposit. *Hubei Geology*, **8**, 60–66 (in Chinese).
Zang, W. and Fyfe, W.S. (1993) A three stage genetic model for the Igarape Bahia lateritic gold deposit, Carajas, Brazil. *Economic Geology*, **88**, 1768–1779.

(*Received 10 October 2003; revised 1 November 2004; Ms. 843; A.E. W. Crawford Elliott*)